Carbohydrate Research, 181 (1988) 23–40
Elsevier Science Publishers B.V., Amsterdam – Printed in The Netherlands

CATION INTERACTIONS IN GELLAN: AN X-RAY STUDY OF THE POTASSIUM SALT

RENGASWAMI CHANDRASEKARAN*, LUIS C. PUIGJANER, KAREN L. JOYCE, AND STRUTHER ARNOTT
The Whistler Center for Carbohydrate Research, Purdue University, West Lafayette, Indiana 47907 (U.S.A.)

(Received November 30th, 1987; accepted for publication in revised form, March 18th, 1988)

ABSTRACT

Gellan belongs to a new generation of nonsulfated, microbial, texturing polysaccharides of potential interest to the food industry. The influence of monovalent cations on its molecular geometry has been investigated by X-ray diffraction analysis of oriented fibers of the potassium salt. The molecule forms a parallel, half-staggered, double helix in which each polysaccharide chain is a left-handed, 3-fold helix of pitch 5.63 nm. The potassium ion is coordinated to the carboxylate group, which is in turn involved in interchain hydrogen-bonds to stabilize the duplex. There are two such duplexes, packed antiparallel to each other, cross-linked by a network of duplex–water–duplex interactions, in the trigonal unit cell, $a = b = 1.575$ nm, and $c = 2.815$ nm. The present study not only confirms the correctness of the basic structure of gellan reported previously for the lithium salt but also furnishes a clear insight into the critical interactions taking place between the polymer chains, cations, and water molecules which are of importance for industrial utilization.

INTRODUCTION

Gellan is one of several new, nonsulfated, texturing and gelling agents which are of interest to the food industry. This microbial polysaccharide forms gels with both monovalent and divalent cations[1,2]. Such physical properties as the setting temperature, strength, and firmness of the gel depend on the type of cation present, as well as its ionic strength. For example, potassium ions set the gels at a lower temperature than calcium ions. On the other hand, the latter can yield gels of the same strength and quality as potassium, but at a much lower concentration, approximately 1/40th that of the monovalent ions. In order to evaluate the molecular basis of the role of cations on the gelling behavior observed, it is necessary to determine the molecular architecture of the polysaccharide chains and the positions of the ions and water molecules relative to them. This should eventually lead to an under-

*To whom correspondence should be addressed.

0008-6215/88/$ 03.50

standing of the various steps involved in the gelling mechanism of this industrially important polysaccharide. The three-dimensional structure of the potassium salt of gellan described herein represents a substantial advancement in our current knowledge of this polymer, and provides a deeper insight into its physicochemical properties.

The basic molecular model of gellan has been the subject of some preliminary X-ray studies[3,4]. The models proposed in these investigations have turned out to be either speculative, or incompatible with the observed X-ray data. Only recently, on the basis of a careful re-analysis of an X-ray diffraction pattern from the lithium salt of gellan, have the main features of the molecule emerged with certainty[5]. The polysaccharide chain forms a left-handed, 3-fold helix of pitch (*P*) 5.64 nm. Two chains are organized parallel so as to form an intertwined double-helix in which one polysaccharide chain is translated by half the pitch, relative to the other, along the common helix-axis.

However, owing to the low X-ray-scattering factor of its cations, the lithium salt of gellan is an unfavorable system to detect cation positions and then to explore the solvent environment. We have now obtained good diffraction patterns from polycrystalline and well-oriented samples of the potassium salt of gellan. Detailed structure analysis has enabled us to determine the positions of the potassium ions and the surrounding periodic water molecules, and their interactions with the polysaccharide chains which are responsible for the observed physical properties of the polymer. This information should enable manipulation of the system for improved industrial utilization.

The results of this study further support the concept that the gellan molecule adopts the double-helical form, as in the lithium case[5], and indicate that one K^+ ion is associated with the carboxylate group in every tetrasaccharide repeating-unit[6,7] consisting of →3)-β-D-Glc*p*-(1→4)-β-D-Glc*p*A-(1→4)-β-D-Glc*p*-(1→4)-α-L-Rha*p*-(1→. Throughout this article, the four residues in the repeating unit are, for convenience, respectively, referred to as A, B, C, and D. Both chains in the double helix participate to provide five ligands for the potassium coordination. This includes the hydroxyl, hydroxymethyl, and carboxylate groups; a water molecule serves as the sixth ligand. All of these ligands are found roughly on the inner surface of the double helix. Additional water molecules serve as bridges to crosslink neighboring double-helices in the crystal structure, and they add stability to the network of molecular aggregates.

EXPERIMENTAL

Sample preparation. — Commercial samples of gellan gum in its deacetylated form (GELRITE) were kindly provided by Dr. Ralph Moorhouse (Kelco Division of Merck & Co., Inc., San Diego, CA). A solution (0.4 mg/mL) was heated with stirring to 82° and held there for 10 min to solubilize the gum. Upon slowly adding, with agitation, the gellan solution to a 0.1M HCl (100 mL) kept at 74°, fully

protonated, noodle-shaped fibers of pure "gellanic acid", free from any cations or other impurities were obtained and were allowed to stand for 3 to 5 min to harden. These fibers were washed repeatedly with distilled water until no trace of HCl could be detected in the wash water, $AgNO_3$ being used to test the presence of chloride ions (indicated by a milky, white precipitate). Finally, the fibers were mashed to a homogeneous fluid in a small amount of distilled water by using a mortar and pestle. A portion (~10 mg) of this sample was converted into the potassium salt form by dialysis against 10mM KF (4 × 250 mL). The excess of salt was removed by further dialysis against distilled water (4 × 250 mL) during 2 days. The polysaccharide was then freeze-dried.

Well oriented and polycrystalline fibers of the K^+ salt of gellan were prepared by using conventional, fiber-pulling techniques. One or more drops of the polysaccharide solution were placed between the two glass rods in a fiber puller and allowed to dry slowly under controlled relative humidity and temperature. During the drying process, the fiber was gradually stretched to about twice its original length. The density of the fiber was measured by the flotation method, using a mixture of bromobenzene and benzene.

X-Ray intensity data. — X-Ray diffraction patterns from well oriented and polycrystalline, fibrous specimens were recorded on flat photographic films, using pin-hole cameras. The film-to-sample distance was typically 55 mm. Nickel-filtered, CuKα radiation (λ 0.15418 nm) from a Philips microfocus generator (operated at 40 kV, 6 mA) was used in the X-ray experiments. The fibers were maintained at the desired relative humidity throughout the exposure by continuously flushing the camera with helium which had previously been passed through an appropriate, saturated salt solution. Calcite (characteristic spacing, 0.3035 nm) dusted fibers were X-rayed for accurate measurement of unit-cell dimensions.

The diffraction pattern was digitized by using an Optronics P-100 rotating-drum microdensitometer with a 100-μm raster. Background correction and structure amplitudes were determined as described.[8,9].

Molecular-model building, and structure analysis. — Polysaccharide chains consistent with the experimentally observed helix symmetry and pitch were constructed by using the method of linked-atom least-squares[10]. Standard sugar geometries were used in the early stages, but were made flexible at the end. The details are essentially the same as reported previously in a study on the Li^+ gellan structure[5]. In addition, three positional parameters (s, μ, and w) were used to define the position of each cation or water molecule, where s is the distance from the helix axis, μ is the orientation about the helix axis, and w is z/c, related to the z-coordinate. The cations and periodic water molecules were located by employing difference Fourier syntheses using $2F_o$-F_c or F_o-F_c as coefficients and phases corresponding to the current model.

Constrained and restrained least-squares refinement of the crystal structures with the polyanion molecules surrounded by the cations and water molecules were finally conducted.

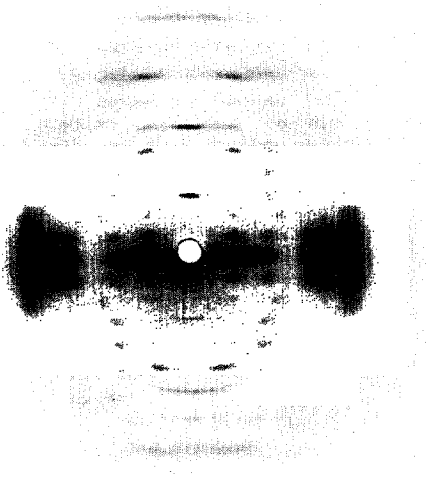

Fig. 1. X-Ray fiber diffraction pattern from a well oriented and polycrystalline sample of the potassium salt of gellan.

DIFFRACTION PATTERN AND UNIT-CELL CONTENTS

The diffraction patterns from fibers of the K^+ salt obtained at relative humidities of 43 to 92% indicated that the specimens were polycrystalline and well oriented. A typical diffraction pattern recorded at 75% relative humidity is shown in Fig. 1. All of the 3 meridional and 38 non-meridional sharp spots could be indexed on the basis of a trigonal unit-cell of dimensions $a = b = 1.575(4)$ nm and $c = 2.815(8)$ nm. This unit cell is isomorphous with that of the Li^+ salt[5]. The X-ray data-set used in the structure analysis also included 13 additional spots whose intensities were too weak to be measured, and a uniform "threshold" value was assigned to each of them. In this category, those spots whose calculated structure-amplitudes were less than the corresponding observed (threshold) amplitudes were rejected from the least-squares refinement.

The general features of the diffraction pattern (see Fig. 1) are similar to those of the Li^+ salt[5], except for the differences visible in intensity modulation throughout the field of view, and an overall higher quality. Consequently, the spots are sharper and well resolved out to 0.28 nm; there are also 2 extra spots on $l = 9$ and 10. The close similarities in the diffraction patterns of the two salts indicated that they have essentially similar molecular structures. It thus follows that the K^+ gellan molecule forms a parallel double-helix in which the two polysaccharide chains of 3-fold, left-handed helix symmetry, and pitch (P) of 5.63 nm, are translated from each other along the common helix-axis by exactly half the pitch.

The measured density of the fiber (1.49 g/mL) is consistent with six tetrasaccharide repeating units in the unit cell, along with a K^+ ion and ~13 water molecules per tetrasaccharide unit.

STRUCTURE ANALYSIS

(*a*) *Choosing the correct packing model.* — By analogy with the crystal structure of Li^+ gellan[5], here also two molecules must be positioned at the points (2/3, 1/3) and (1/3, 2/3) in the *ab* plane with their molecular axes along [001]. Because $P = 2\ c$, any unit cell will therefore contain only half a pitch length of the molecule in height *c* at each site, so that a *c*-translation will lead to the other half of the pitch in the adjoining unit-cell. Two molecules can be packed in the unit cell in one of three different ways, using two orientational parameters μ_1 and μ_2 and a translational parameter w_2 (expressed as a fraction of *c*) of the second molecule along its helix axis relative to the first. The packing can be either parallel (Model 1) or antiparallel (Model 2). Both require all three parameters (μ_1, μ_2, and w_2) as variables, and correspond to the space group $P3_1$. The third choice (Model 3) is to exploit a crystallographic dyad along the short diagonal [110] in the antiparallel case. This lowers the number of variables to two (μ_2 and w_2), and leads to the space group $P3_121$. It may be noted that the symmetry of the polysaccharide chain is 3_2 in all these cases, but that of the molecular double-helix is 3_1, the same as the space-group symmetry.

We tested all three possibilities by conducting a series of experiments to ascertain their relative merits. Treating the double helix as a rigid body, μ_1, μ_2, and w_2 were varied stepwise in the three-dimensional (μ_1, μ_2, w_2) space, and the X-ray (*X*), the steric compression (*C*) terms[5], and the crystallographic *R* value were computed at each grid point. Next, the minima in each of these surveys were used as the starting values for subsequent refinements of the crystal structures. In these refinements, the variable parameters in the tetrasaccharide asymmetric unit were the two conformation angles (ϕ, ψ) around each glycosidic bond and the torsion angles defining the orientations of the hydroxymethyl, carboxylate, and methyl side-chains.

Statistics of the best-refined crystal structure for each of the three packing models are given in Table I. In comparing any two models, it should be borne in mind that the magnitudes of *X* and *C* respectively quantify the extent of disagreement for the X-rays and steric acceptance. In other words, smaller numbers are

TABLE I

COMPARISON OF THE THREE CRYSTAL-STRUCTURE MODELS POSSIBLE FOR THE 3-FOLD POTASSIUM SALT OF GELLAN AFTER REFINEMENT AGAINST X-RAY DATA AND CONTACTS

Model	*Space group*	*Packing*	X[a]	C[a]	R[a]
1	$P3_1$	parallel	34	111	0.36
2	$P3_1$	antiparallel	30	98	0.30
3	$P3_121$	antiparallel	35	184	0.40

[a] *X* and *C* are respectively the X-ray and contact terms in the optimization function which is minimized by the least-squares procedure[10], and *R* is the crystallographic reliability index.

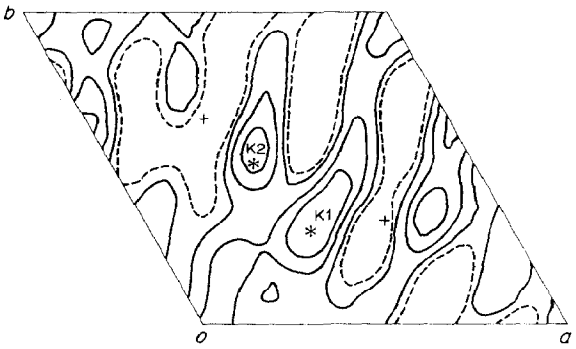

Fig. 2. Section of three-dimensional, difference electron-density map at level $z = -c/12$, showing the locations of potassium ions K1 and K2.

more acceptable. Thus, the high symmetry space group $P3_121$ (Model 3) can be decisively eliminated. Similarly, the parallel packing (Model 1) is also inferior. The $P3_1$ antiparallel packing (Model 2) is indeed the best for satisfying both the X-ray data and the steric observations remarkably well, and, by using the Hamilton significance test[11], can be ranked as the correct representation of the crystal structure of K^+ gellan. Furthermore, this confirms the robustness of the polysaccharide chains and of the favored packing-arrangement deduced in the Li^+ gellan crystal structure[5].

(*b*) *Location of cations and water molecules.* — Difference-Fourier maps (see Fig. 2) were computed for Model 2 by using normal, atomic-scattering factors[12]. Because the two double-helices in the unit cell are not related by a crystallographic dyad, the regions surrounding both molecules in 1/3 of the unit cell, which constitutes the crystallographic asymmetric unit, were carefully examined. The main additional density, and therefore the most probable K^+ site for one, was found in the vicinity of a carboxylate group, and 3 other polyanion oxygen atoms within corrdinating distances. As expected, a similar situation was realized for the second molecule also.

Potassium ions (K1 and K2) were placed at these two locations, and their positions, as well as the molecular and packing parameters of the polyanion, and the X-ray scale-factor were simultaneously refined. A second difference-Fourier map, using the refined structure as the new phasing model, revealed two water sites, W1 near K1, and W2 near K2. Further refinements of the augmented crystal structure, with the two K^+ ions and the two water molecules, followed by difference-Fourier maps, resulted in identifying six more water molecules, three of them relating polyanion oxygen atoms of neighboring, antiparallel chains. Attempts to locate additional periodic scatterers were, however, unsuccessful.

At this stage, the crystallographic residual R for the polyanions alone was 0.42, corresponding to the use of conventional, atomic-scattering factors[12]. On the other hand, as Table I shows, the X-ray agreement was so much better ($R = 0.30$)

TABLE II

CARTESIAN AND CYLINDRICAL POLAR COORDINATES FOR AN ASYMMETRIC UNIT OF THE POTASSIUM SALT OF GELLAN CONSISTING OF A TETRASACCHARIDE[a] IN ONE CHAIN, THE ASSOCIATED CATIONS, AND WATER MOLECULES

Group	Atom	X(NM)	Y(NM)	Z(NM)	R(NM)	PHI(DEG)
Residue A	C-1	-0.1524	-0.3063	1.5022	0.3421	-116.45
	C-2	-0.1344	-0.2586	1.6458	0.2914	-117.45
	C-3	-0.1874	-0.3624	1.7435	0.4080	-117.35
	C-4	-0.3314	-0.3978	1.7087	0.5178	-129.80
	C-5	-0.3417	-0.4378	1.5619	0.5553	-127.97
	C-6	-0.4843	-0.4632	1.5181	0.6702	-136.27
	O-1	-0.1146	-0.2033	1.4170	0.2334	-119.41
	O-2	0.0035	-0.2325	1.6697	0.2325	-89.15
	O-3	-0.1797	-0.3112	1.8767	0.3584	-120.00
	O-4	-0.3766	-0.5067	1.7889	0.6313	-126.62
	O-5	-0.2906	-0.3332	1.4778	0.4421	-131.10
	O-6	-0.5299	-0.5923	1.5584	0.7947	-131.81
	H-1	-0.0938	-0.3981	1.4866	0.4090	-103.26
	H-2	-0.1883	-0.1638	1.6600	0.2496	-138.98
	H-3	-0.1250	-0.4526	1.7352	0.4696	-105.44
	H-4	-0.3962	-0.3109	1.7278	0.5036	-141.88
	H-5	-0.2839	-0.5298	1.5449	0.6010	-118.18
	H-61	-0.5501	-0.3861	1.5608	0.6721	-144.94
	H-62	-0.4912	-0.4545	1.4087	0.6692	-137.23
Residue B	C-1	0.0634	-0.1661	1.0431	0.1777	-69.12
	C-2	-0.0521	-0.2650	1.0530	0.2700	-101.12
	C-3	-0.1341	-0.2363	1.1778	0.2717	-119.57
	C-4	-0.0428	-0.2410	1.2997	0.2448	-100.08
	C-5	0.0746	-0.1456	1.2805	0.1635	-62.88
	C-6	0.1753	-0.1535	1.3932	0.2330	-41.20
	O-1	0.1417	-0.2013	0.9340	0.2462	-54.86
	O-2	-0.1321	-0.2557	0.9357	0.2878	-117.33
	O-3	-0.2382	-0.3334	1.1901	0.4098	-125.54
	O-4	-0.1146	-0.2033	1.4170	0.2334	-119.41
	O-5	0.1455	-0.1765	1.1595	0.2287	-50.49
	O-61	0.1612	-0.2465	1.4755	0.2945	-56.82
	O-62	0.2650	-0.0664	1.3954	0.2732	-14.07
	H-1	0.0233	-0.0639	1.0355	0.0680	-69.95
	H-2	-0.0123	-0.3674	1.0571	0.3676	-91.92
	H-3	-0.1806	-0.1370	1.1692	0.2267	-142.81
	H-4	-0.0048	-0.3435	1.3113	0.3436	-90.79
	H-5	0.0373	-0.0422	1.2754	0.0563	-48.49
Residue C	C-1	0.1936	-0.0860	0.5430	0.2118	-23.95
	C-2	0.1574	0.0273	0.6380	0.1598	9.85
	C-3	0.1837	-0.0186	0.7806	0.1847	-5.77
	C-4	0.1043	-0.1455	0.8082	0.1790	-54.38
	C-5	0.1319	-0.2508	0.7014	0.2834	-62.26
	C-6	0.0433	-0.3728	0.7152	0.3753	-83.38
	O-1	0.1678	-0.0451	0.4127	0.1738	-15.05
	O-2	0.2337	0.1428	0.6048	0.2738	31.43
	O-3	0.1454	0.0844	0.8720	0.1682	30.13
	O-4	0.1417	-0.2013	0.9340	0.2462	-54.86
	O-5	0.1080	-0.1971	0.5704	0.2248	-61.27
	O-6	-0.0951	-0.3388	0.7079	0.3519	-105.69
	H-1	0.2984	-0.1158	0.5582	0.3201	-21.20
	H-2	0.0514	0.0536	0.6251	0.0743	46.23
	H-3	0.2912	-0.0379	0.7937	0.2937	-7.41
	H-4	-0.0028	-0.1205	0.8096	0.1205	-91.35
	H-5	0.2366	-0.2839	0.7087	0.3695	-50.19
	H-61	0.0675	-0.4450	0.6359	0.4501	-81.37
	H-62	0.0638	-0.4224	0.8112	0.4272	-81.41
Residue D	C-1	0.4308	0.0609	0.1044	0.4351	8.04
	C-2	0.3446	0.1699	0.1667	0.3842	26.25
	C-3	0.2244	0.1065	0.2353	0.2484	25.39
	C-4	0.2776	0.0127	0.3427	0.2779	2.62
	C-5	0.3640	-0.0949	0.2754	0.3762	-14.62
	C-6	0.4291	-0.1902	0.3739	0.4594	-23.90
	O-1	0.3594	0.0000	0.0000	0.3594	0.00
	O-2	0.4256	0.2415	0.2588	0.4893	29.57
	O-3	0.1449	0.2121	0.2857	0.2568	55.66
	O-4	0.1678	-0.0451	0.4127	0.1738	-15.05
	O-5	0.4715	-0.0332	0.2026	0.4727	-4.02
	H-1	0.5197	0.1052	0.0571	0.5302	11.45
	H-2	0.3108	0.2392	0.0882	0.3922	37.59
	H-3	0.1656	0.0501	0.1615	0.1730	16.83
	H-4	0.3396	0.0704	0.4129	0.3468	11.70
	H-5	0.3022	-0.1532	0.2055	0.3388	-26.89
	H-61	0.3545	-0.2625	0.4098	0.4411	-36.52
	H-62	0.5113	-0.2438	0.3242	0.5664	-25.50
	H-63	0.4689	-0.1332	0.4592	0.4874	-15.85
K + Solvent	K-1	-0.2852	0.1038	-0.1757	0.3129	160.63
	K-2	-0.4192	0.5025	-0.2488	0.6544	129.84
	W-1	0.0293	-0.3660	1.0183	0.3672	-85.42
	W-2	-0.3195	0.5733	-0.4554	0.6563	119.13
	W-3	-0.4508	0.9911	-0.6858	1.0888	114.46
	W-4	-0.9305	0.9683	-0.3593	1.3429	133.86
	W-5	0.2149	-0.0257	0.2408	0.2165	-6.81
	W-6	0.4542	-0.6128	-0.3144	0.7628	-53.45
	W-7	-0.6965	0.2794	-0.4478	0.7505	158.14
	W-8	-0.5015	-0.3253	-0.0267	0.5541	154.79

TABLE III

STRUCTURE AMPLITUDES[a] FOR THE POTASSIUM SALT OF GELLAN

A Scaled observed amplitudes F_O

H K	L=0	1	2	3	4	5	6	7	8	9	10
0 0	M	N	N	M	N	N	M	N	N	M	N
1 0	345	171	84	49	52	115	73	93	146	97	185
1 1	246	147	(61)	90	92	112	53	76			
2 0	191	134	106	(68)	(72)	(72)	96	(54)	227		
2 1	448	331	173	125	143	143	164	107			
3 0	531	409	238	150	(90)	(109)	(109)	(79)			
2 2 3 1	767	672	406	(178)							
4 0	(150)	(135)	(89)								

B Calculated structure amplitudes F_C

H K	L=0	1	2	3	4	5	6	7	8	9	10
0 0	(949)	0	0	(107)	0	0	(117)	0	0	(150)	0
1 0	396	256	111	100	94	81	82	88	145	109	184
1 1	208	205	(152)	139	96	89	128	75			
2 0	192	80	124	(116)	(116)	(83)	155	(110)	212		
2 1	432	340	182	123	124	136	215	183			
3 0	541	335	237	160	(90)	(93)	(157)	(89)			
2 2 3 1	654	565	410	(223)							
4 0	(164)	(117)	(115)								

[a]Amplitudes in parentheses indicate reflections below the threshold of observation, and their estimated threshold values are given in A. Such reflections were only included in the refinement when the calculated amplitudes were greater than the threshold. M and N denote meridional and systematically absent reflections, respectively. An isotropic attenuation factor exp $(-0.06 \sin^2\theta/\lambda^2)$, where $\lambda = 0.15418$ nm, was applied to the calculated amplitudes in all the structure-factor calculations.

[a]The next two tetrasaccharides in the chain are generated as $(R, \phi - 120°, Z + 2c/3)$, and $(R, \phi + 120°, Z + 4c/3)$. The second chain in the double helix can be generated from the first by adding c to the corresponding Z coordinates. The asymmetric unit of the down-pointing molecule (II) at (1/3, 2/3) in the unit cell will have $(R, -\phi, Z)$ for its atomic coordinates. The crystal structure can be derived from these molecular coordinates by applying the packing parameters μ_1 for the "up", and (μ_2, w_2) for the "down" molecules I and II in the unit cell, 75.2° and (5.4°, −0.1532) respectively. Cylindrical polar coordinates for cation and water molecules belonging to both double-helices are, however, provided relative to those of the polyanion helix I at (2/3, 1/3).

when the water-weighted scattering-factors[13], on the basis of solvent (water) electron density equal to 298.4 e/nm^3, were used. Thus, it may be suspected that most of the untraceable scattering material in the unit cell is non-periodic. In fact, the 4 periodic water molecules per tetrasaccharide repeat located in the difference-Fourier maps constitute less than one-third of the 13 water molecules expected from density measurement. This rationalizes use of water-weighted scattering-factors in further calculations, and justifies the accountability of the remaining, unlocated scattering-material as being smeared throughout the interstitial space.

The final refinement-procedure involved two major steps. First, the conformation angles (ϕ, ψ, χ) of the polyanions and their relative positional parameters (μ_1, μ_2, and w_2) were allowed to vary, although elastically tethered to appropriate standard values wherever relevant, together with the positions of each cation and water molecule added to the system. In the second step, the glycosidic-bridge bond angles, as well as the endocyclic conformation and bond angles of the pyranose rings, which were all held rigid hitherto, were also allowed to relax; this raised the total number of variable parameters to 74. At the completion of the X-ray refinement, the final crystal structure has an R value of 0.18 for the entire data set, consisting of 51 spots. All the potential functional groups participate in hydrogen bonds. The atomic coordinates are given in Table II. The observed and calculated structure amplitudes are listed in Table III.

STRUCTURAL FEATURES

(*a*) *Polyanion conformation.* — The molecule exists as a double helix. The major conformation angles (ϕ, ψ) around the glycosidic bridges, and χ around the

TABLE IV

FINAL VALUES OF THE MAJOR CONFORMATIONAL ANGLES (AND ESD VALUES) OF THE POTASSIUM SALT OF GELLAN, COMPARED WITH THOSE OF THE LITHIUM SALT[5].

Conformation angle	*Value (°)*		*Comments*
	Potassium salt	*Lithium salt*	
ϕ_1(O5D-C1D-O3A-C3A)	−124 (2)	−140	α-(1→3)
ψ_1(C1D-O3A-C3A-C4A)	88 (3)	105	α-(1→3)
χ_1(C4A-C5A-C6A-O6A)	−79 (9)	−66	hydroxymethyl
ϕ_2(O5A-C1A-O4B-C4B)	−101 (3)	−86	β-(1→4)
ψ_2(C1A-O4B-C4B-C5B)	−136 (2)	−140	β-(1→4)
χ_2(C4B-C5B-C6B-O61B)	10 (6)	−8	carboxylate
ϕ_3(O5B-C1B-O4C-C4C)	−154 (3)	−150	β-(1→4)
ψ_3(C1B-O4C-C4C-C5C)	−144 (2)	−134	β-(1→4)
χ_3(C4C-C5C-C6C-O6C)	58 (6)	53	hydroxymethyl
ϕ_4(O5C-C1C-O4D-C4D)	−150 (4)	−168	β-(1→4)
ψ_4(C1C-O4D-C4D-C5D)	86 (3)	75	β-(1→4)
χ_4(C4D-C5D-C6D-H61D)	77 (6)	88	methyl

C-5–C-6 bond, for each sugar residue in a tetrasaccharide repeating-unit are listed in Table IV. The corresponding values determined for the Li^+ salt[5] are also provided for comparison. The pyranose ring geometries are fairly standard; no individual conformation angle deviates by more than 5°, the mean departure being only 1.9°, from that of the $^4C_1$ (D-glucose and D-glucuronate) and $^1C_4$ (L-rhamnose) conformations. Similarly, the endocyclic and glycosidic-bridge bond angles in the polymer chains have scarcely deviated from the expected values; the maximum individual deviation is 1.8°, and the average deviation is a nominal 0.6°.

The molecule is remarkably slim and extended. The carboxylate group of each glucuronate residue is rotated by 9.5° with respect to its C-4–C-5–C-6 plane. In the tetrasaccharide repeating unit, the hydroxymethyl groups of the two D-glucose residues have quite different conformations: $\chi_1 = -79°$ and $\chi_3 = 58°$. This trend is essential for the formation of intra- and inter-chain hydrogen-bonds.

Because of the intrusion of the α-(1→3) linkage between rhamnose D and glucose A residues in a cellulose-like polymer, concomitant morphological bulges are apparent. Scanning the radial atomic coordinates (see Table II) indicate that both A and D, at $r = 0.79$ nm and 0.57 nm, respectively, describe the periphery of the double helix; in contrast, both glucuronate B and glucose C are located quite close to the helix axis, and form the inner core. Consequently, as will be shown, these two residues are crucial for the interchain association and, hence, double helix formation.

The consequences of the α-(1→3) linkage are further seen in the secondary structure. The turn angle of −120° for a tetrasaccharide is not evenly distributed among the 4 residues. The 4 local turn angles, calculated as the differences in the cylindrical polar angles ϕ of adjacent bridge-oxygen atoms (see Table II), are dramatically different from each other. The "bulged out" residues glucose A (−0.5°) and rhamnose D (−15°) turn around the helix axis much less than the average value of −30° per residue. On the contrary, the other two "buried in" residues, glucuronate B (−65°) and glucose C (−40°), have considerably greater than the average turn angle, and provide the compensation needed. A similar trend in the projected lengths of adjacent bridge-oxygen atoms along the helix axis also deserves mention, namely, larger values for glucuronate B (0.48 nm) and glucose C (0.52 nm) than for rhamnose D (0.41 nm) and glucose A (0.46). In the fully extended cellulose, this axial rise is[14] 0.52 nm.

It is of interest to point out that only at the linkage between residues A and B (see Table IV) do the conformation angles (ϕ_2, ψ_2) match fairly well with those (−98°, −142°) of cellulose[14].

(*b*) *Intra-chain hydrogen bonds.* — Because of the resemblance of (ϕ_2, ψ_2) to that in cellulose, the gellan chain also has the O3B···O5A bond across the (1→4) linkage. This stability is further enhanced by two other hydrogen bonds O2A···O61B and O2B··O6C (see Table V).

(*c*) *Inter-chain hydrogen bonds.* — The double helix is formed by the association of two conformationally identical polysaccharide chains of the same polarity

TABLE V

ATTRACTIVE INTERACTIONS INVOLVING THE POLYANION, POTASSIUM IONS, AND WATER MOLECULES[a] IN THE CRYSTAL STRUCTURE OF THE POTASSIUM SALT OF GELLAN

Type	*Atom*[b] *X*	*Atom Y*	*Distance (nm)*	*Precursor (P)*	*Angle (degrees) P-X···Y*
Intrachain	O3B	O5A	0.292	C3B	102
	O2A	O61B	0.251	C2A	118
	O2B	O6C	0.245	C2B	131
Interchain	O6C	O62B	0.304	C6C	117
Inter double helix	O4A(II)	O6A(I)	0.286	C4A	122
	O2D(II)	O3B(I)	0.253	C2D	136
	O2D(I)	O5B(II)	0.256	C2D	132
Potassium coordination	O2A(I,2)	K1	0.262	C2A	177
	O61B(I,2)	K1	0.255	C6B	110
	O62B(I,2)	K1	0.325	C6B	76
	O2B(I,1)	K1	0.260	C2B	155
	O6C(I,1)	K1	0.283	C6C	144
	W1	K1	0.264		
	O2A(II,1)	K2	0.256	C2A	171
	O61B(II,1)	K2	0.253	C6B	105
	O62B(II,1)	K2	0.311	C6B	77
	O2B(II,2)	K2	0.247	C2B	155
	O6C(II,2)	K2	0.261	C6C	140
	W2	K2	0.240		
Water bridges					
Intra-chain	O2B(II,2)	W7	0.276	C2B	100
	O3B(II,2)	W7	0.286	C3B	113
Inter-chain	O2B(I,1)	W1	0.266	C2B	103
	O3D(1,2)	W1	0.265	C3D	108
	O62B(I,2)	W5	0.309	C6B	103
	O3C(I,2)	W5	0.312	C3C	136
	O4D(I,1)	W5	0.278	C4D	120
	O2A(II,1)	W2	0.269	C2A	130
	O2B(II,2)	W2	0.271	C2B	103
	O3D(II,1)	W2	0.264	C3D	76
	O62B(II,2)	W3	0.308	C6B	100
	O3C(II,2)	W3	0.304	C3C	135
	O4D(II,1)	W3	0.278	C4D	122
Inter double helix	O4C(II,2)	W4	0.301	C4C	141
	O2C(I,2)($\bar{1}$00)	W4	0.297	C2C	136
	O6A(I,1)($\bar{1}$00)	W6	0.270	C6A	157
	O4A(II,1)(0$\bar{1}$0)	W6	0.296	C4A	139
	O6A(II,1)(0$\bar{1}$0)	W6	0.258	C6A	143
	W7	W6	0.272		
	O2B(I,2)	W8	0.273	C2B	97
	O6C(I,2)	W8	0.289	C6C	98
	O2C(II,2)(0$\bar{1}$0)	W8	0.288	C2C	154
	O2D(II,2)(0$\bar{1}$0)	W8	0.282	C2D	144

[a]The "up" and "down" molecules are distinguished by I and II, and, similarly, the two chains in each duplex by 1 and 2, within parentheses. Molecules outside the reference unit-cell are designated by the appropriate unit-cell translations in the double helix–water–double helix interactions under the type inter double helix. [b]X is the donor atom, Y is the acceptor, and P is the non-hydrogen atom covalently linked to X.

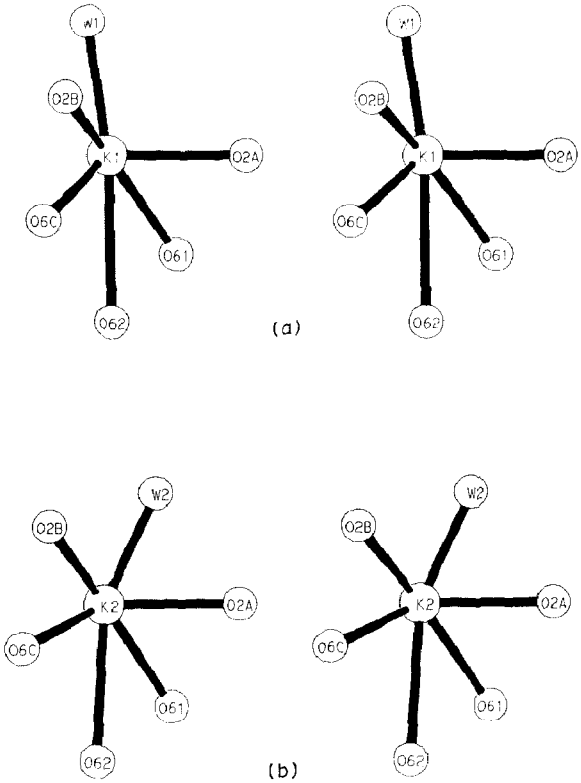

Fig. 3. Coordination of the potassium ions shown in stereo (a) K1 and (b) K2. [Five ligands are from the polyanion duplex, and one is from a water molecule. The six ligands constitute a distorted octahedron around the potassium ion in the middle.]

about the common helix axis, such that one is longitudinally translated half a pitch-length from the other. In this process, the internally buried glucuronate B and glucose C residues on opposite strands are brought into juxtaposition. This facilitates an inter-chain hydrogen-bond O6C···O62B (see Table V) which happens to be the major driving-force for the stability of the double helix. In this context, it is relevant to mention that O6C has a key structural role in the gellan architecture. Only in the g^+ domain for χ_3 is O6C suitably positioned to make the inter-chain hydrogen-bond, as well as the short (0.245 nm) intra-chain O2B···O6C hydrogen-bond. In the other two (g^- and t) staggered domains, as indicated by the present and previous[5] model-building studies, O6C will not be able to make either of them, and this might disrupt the stability of the system.

(*d*) *Binding of potassium ions and water molecules.* — The two potassium ions in the asymmetric part of the unit cell, K1 and K2, are related by a pseudo-dyad. This is located at ~10° away from the short diagonal [110], and does not coincide with the dyad relating the two double-helices. Hence, the coordination

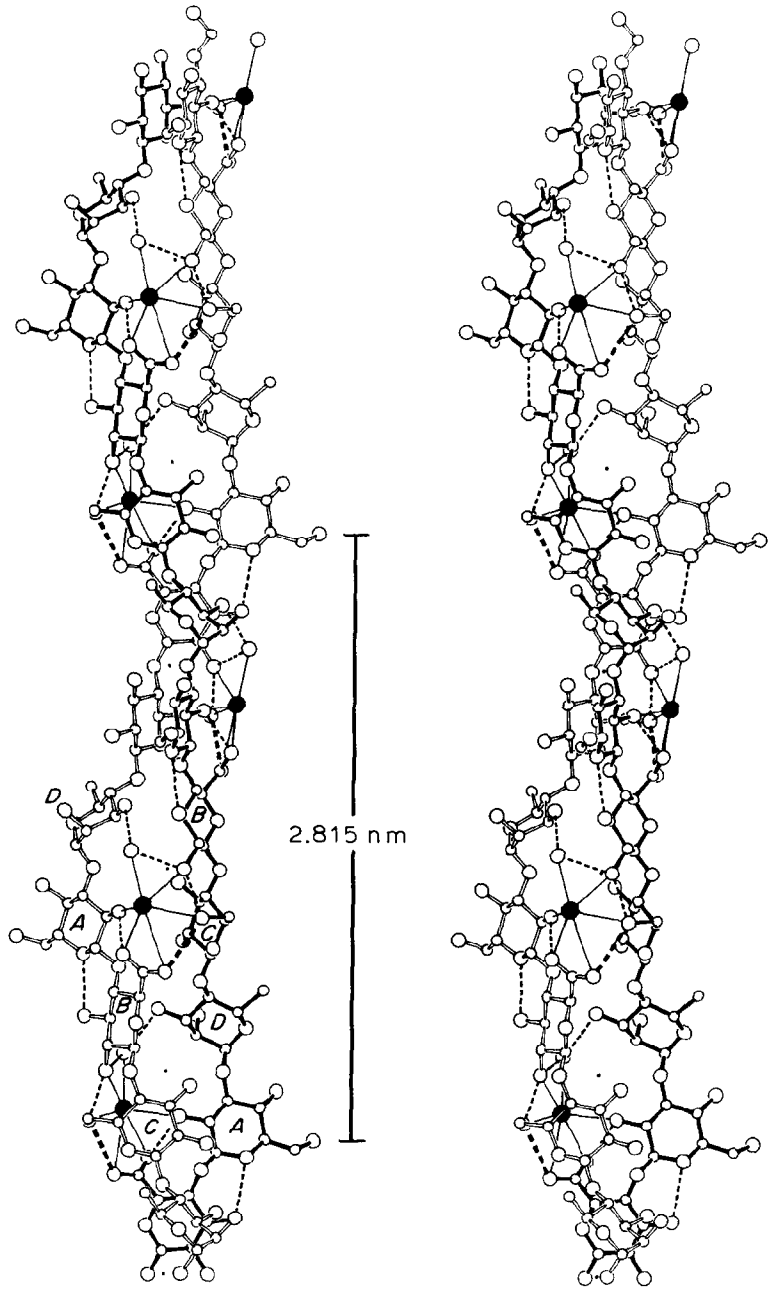

Fig. 4. A stereo drawing of the gellan double helix and the coordinating potassium ions (filled circle) and water molecules (open circle). [The hydrogen bonds within a chain (thin dashed lines), and between the chains (thick dashed lines), are shown, along with the six ligands attached to the potassium ion (thin line).]

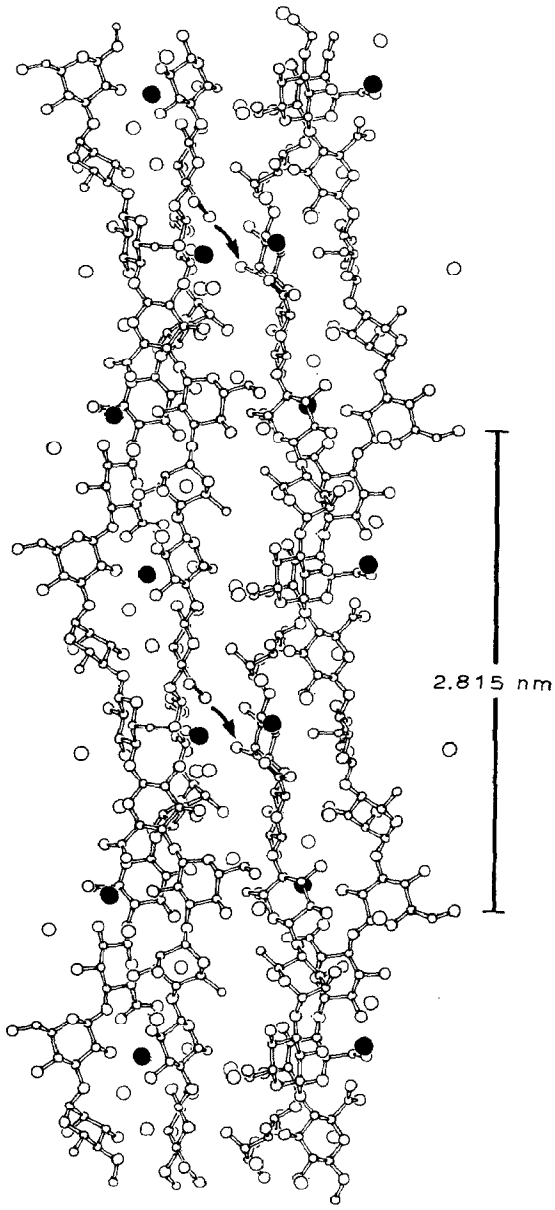

Fig. 5. Packing of two adjacent, up and down, gellan molecules, the potassium ions, and the water molecules coordinated to them in the unit cell viewed along the [110] direction. [The potassium ions and water molecules are shown by filled and open circles, respectively.]

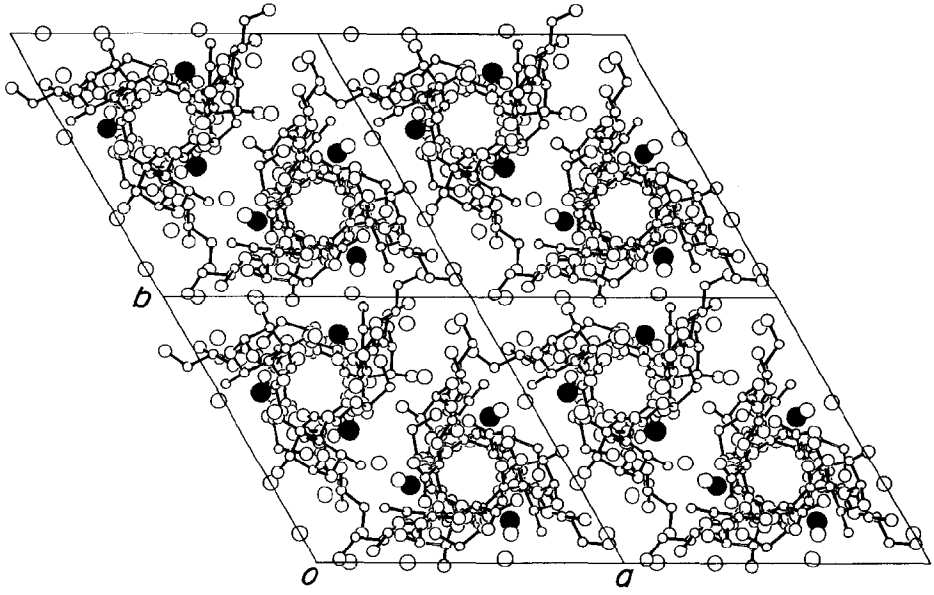

Fig. 6. A *c*-axis projection of the crystal structure. [The potassium ions are drawn in filled circles and water molecules in open circles.]

geometry of K1 is not identical, but is grossly similar, to that of K2 (see Fig. 3). For example, the coordination shell of K1 in molecule I consists of a water molecule W1 and 5 polyanion oxygen atoms, *viz.*, the two charged carboxylate oxygen atoms of glucuronate B and O2A of one strand, and O2B and O6C of the second. As may be seen in Fig. 3a, it is clearly a distorted, octahedral coordination and is reminiscent of those reported in other polysaccharide structures[15,16]. Ion K2 in molecule II has essentially the same kind of coordination, involving a water molecule W2 and the five polyanion oxygen atoms of its two strands (see Fig. 3b). The coordinating distances for both ions are listed in Table V. In either case, the water molecule W (*i.e.*, W1 or W2) which completes the octahedron also forms a water bridge across the two strands of the double helix by means of hydrogen bonds, O3D···W and W···O2B, and imparts further stability to the system. In addition, W2 also forms another hydrogen bond with O2A on the strand containing the O3D atom, to which it is already hydrogen-bonded. A similar hydrogen-bond is not, however, made by W1.

Among the six coordinating distances for either potassium ion, that involving O62B is noticeably long, 0.325 and 0.311 nm, respectively, for K1 and K2. Observations of this type are, however, not uncommon[15].

The potassium-ion interactions with the gellan double helix and the first-shell water molecule are illustrated in Fig. 4.

(*e*) *Molecular packing.* — The two molecules, I and II, in the unit cell (see Fig. 5) are stabilized by intermolecular hydrogen-bonds between the free hydroxyl

groups of rhamnose and the functional groups of glucuronate residues. In addition, there is a hydrogen bond between the hydroxymethyl group of glucose A which describes the molecular periphery and O4A of a neighboring molecule. Thus, every molecule in the crystal structure interacts with three nearest-neighbors of opposite polarity, each separated by 0.91 nm, as shown in Fig. 6.

Surrounding the double helices, six additional, periodic water molecules, W3 to W8, are located in the crystallographic asymmetric part of the unit cell, 3 per tetrasaccharide repeat. Each of them is anchored in position by at least two hydrogen bonds with oxygen atoms in the polyanions (see Table V). Altogether, the eight water molecules, W1 to W8, may be classified under three general categories, depending on their function. For example, as in the case of W1 and W2, both W3 and W5 are involved in establishing water bridges across the two polysaccharide chains within the double helix. In contrast, W7 crosslinks, through hydrogen bonds, the atoms O2B and O3B belonging to the same sugar residue. The other three water molecules, W4, W6, and W8, strengthen the intermolecular interactions by the formation of a series of double helix···water···double helix hydrogen-bonds and ensure stability to the crystal structure (see Fig. 6).

DISCUSSION

In the potassium salt of gellan, the polyanion is conformationally quite similar to that found for the lithium salt, and no conformation angle (see Table IV) exhibits more than an 18° difference between the two. The double helix is similar to some of the other gel-forming polysaccharides[17,18]. Although the polysaccharide chain has an extended, cellulose-like conformation, intrachain hydrogen-bonds involving D-glucose and D-glucuronate residues help retain rigidity. The interchain hydrogen-bonds between D-glucuronate and D-glucose C residues strengthen the double helix. However, the durable cohesion of the double helices resides essentially in the binding action of embedded cations and, likewise, water molecules surrounding the polyanion structure.

The fairly tight packing-arrangement of molecules in the potassium, as well as lithium, crystal structure (see Fig. 6) may be due to the strong interactions involving the carboxylate groups in the interior that maximize direct cation–polyanion interactions. In fact, the cations are suitably located so as to coordinate with the polar groups of the polyanion near the carboxylate groups, while the remainder of the double helix interior consists mainly of relatively nonpolar carbon and hydrogen atoms. Furthermore, these cations do seem to have an indirect role in crosslinking the double helices, with the help of water molecules. Although the potassium ions are bound to the interior of the double helix, any given potassium ion in the crystal structure always finds another liganded to a neighboring molecule such that the two are in close proximity for short-range interactions. This can be easily visualized from Fig. 5, where the cations are approximately lined up in horizontal sections having an 0.94-nm vertical separation between consecutive sections.

Every third section, indicated by an arrow mark in Fig. 5, represents this situation, where the pair of cations is separated by just 0.43 nm. This distance is ideally suited for a water molecule, not necessarily periodic but amorphous as it turns out in this case, to form a hydrogen-bond bridge between the two cations. The propagation of this type of polyanion–cation–water–cation–polyanion linkage could be one of the influencing factors for gel formation.

This led to the desire to address the role of divalent cations on gelation properties. An important feature of the crystal structure pertains to the relative positioning of the carboxylate groups in adjacent double helices around this region. They point towards each other in such a way that the oxygen atoms O61B of the two molecules are separated by only 0.51 nm. Judging from the presence of the organized functional groups and the water molecules in the vicinity (see Figs. 5 and 6), this logically appears to be the most probable divalent cation binding-site in a packing arrangement similar to that in the present case. A single divalent cation might readily replace two monovalent cations, and bind to these two carboxylate groups. As a result, divalent cations might establish direct polyanion–cation–polyanion interactions. Intuitively, these interactions would be much stronger than those involving the monovalent cations, where two cations and a water molecule are required to set up similar intermolecular interactions. A few direct crosslinks of this type might be adequate to keep the molecular aggregates from falling apart. This might explain, at least partly, the reported 40-fold diminution in divalent-ion concentration compared to that of the monovalent ions[1,2].

The stability of the crystal structure of the potassium salt is also derived from the various, water-mediated linkages of the forms polyanion–water–polyanion, polyanion–water–water–polyanion, and polyanion–cation–water–polyanion (see Table V). It is possible that the system contains isolated cations surrounded by water molecules, although the presence of large proportions of disordered solvent may mask the clarity of the diffraction data. This is consistent with the experimental observation, and might explain our inability to locate such counterions in detail.

The cohesion offered by this packing arrangement between double helices and within the double helix is important to explain the properties of gels. The gelling mechanism of gellan may be based on the formation of a three-dimensional network of double-helical junction-zones, as proposed for some gel-forming polysaccharides[19]. This mechanism requires the supporting of elastic binding action of appropriate hydrogen-bonded molecules. Thus, the exact location of counterions and its role in shaping the molecular arrangement gives a further insight on the properties and possible manipulation of this important polysaccharide for industrial use.

ACKNOWLEDGMENTS

We thank Deb Zerth for word-processing the manuscript, and Robert Werberig for photography. This study was supported by grants from Kelco (No. 1271670) and the National Science Foundation (No. 8606942).

REFERENCES

1 H. GRASDALEN AND O. SMIDSRØD, *Polymers*, 7 (1987) 371–394.
2 V. CRESCENZI, M. DENTINI, AND T. COVIELLO, *Carbohydr. Res.*, 149 (1986) 425–432.
3 P. T. ATWOOL, E. D. T. ATKINS, C. UPSTILL, M. J. MILES, AND V. J. MORRIS, in G. O. PHILLIPS, D. J. WEDLOCK, AND P. A. WILLIAMS (Eds.), *Gums and Stabilizers for the Food Industry. 3.* Elsevier, London, 1986, pp. 135–145.
4 C. UPSTILL, E. D. T. ATKINS, AND P. T. ATWOOL, *Int. J. Biol. Macromnol.*, 8 (1986) 275–288.
5 R. CHANDRASEKARAN, R. P. MILLANE, S. ARNOTT, AND E. D. T. ATKINS, *Carbohydr. Res.*, 175 (1988) 1–15.
6 M. A. O'NEILL, R. R. SELVENDRAN, AND V. J. MORRIS, *Carbohydr. Res.*, 124 (1983) 123–133.
7 P. E. JANSSON, B. LINDBERG, AND P. A. SANDFORD, *Carbohydr. Res.*, 124 (1983) 135–139.
8 R. P. MILLANE AND S. ARNOTT, *J. Appl. Crystallogr.*, 18 (1985) 419–423.
9 R. P. MILLANE AND S. ARNOTT, *J. Macromol. Sci. Phys.*, *B*24 (1985) 193–227.
10 P. J. C. SMITH AND S. ARNOTT, *Acta Crystallogr., Sect. A*, 34 (1978) 3–11.
11 W. C. HAMILTON, *Acta Crystallogr.*, 18 (1965) 502–510.
12 *International Tables for X-Ray Crystallography*, Vol. IV, Kynoch Press, England, 1974.
13 S. ARNOTT, R. CHANDRASEKARAN, A. W. DAY, L. C. PUIGJANER, AND L. M. WATTS, *J. Mol. Biol.*, 149 (1981) 489–505.
14 K. H. GARDNER AND J. BLACKWELL, *Biopolymers*, 13 (1974) 1975–2001.
15 R. P. MILLANE, A. K. MITRA, AND S. ARNOTT, *J. Mol. Biol.*, 169 (1983) 903–920.
16 A. K. MITRA, S. ARNOTT, R. P. MILLANE, S. RAGHUNATHAN, AND J. K. SHEEHAN, *J. Macromol. Sci. Phys.*, *B*24 (1986) 21–38.
17 S. ARNOTT, W. E. SCOTT, D. A. REES, AND C. G. A. MCNAB, *J. Mol. Biol.*, 90 (1974) 253–267.
18 S. ARNOTT, A. FULMER, W. E. SCOTT, I. C. M. DEA, R. MOORHOUSE, AND D. A. REES, *J. Mol. Biol.*, 90 (1974) 269–284.
19 D. A. REES, I. W. STEELE, AND F. B. WILLIAMSON, *J. Polym. Sci., Part C*, (1969) 261–276.